FULL TITLE
ASP Conference Series, Vol. **VOLUME**, **YEAR OF PUBLICATION**
NAMES OF EDITORS

The Heliosphere as a Probe of Small Scale Structure

P. C. Frisch

University of Chicago, Department of Astronomy and Astrophysics

Abstract. The heliosphere serves as a probe of interstellar material (ISM) close to the Sun. Measurements of ISM inside and outside of the heliosphere show that we reside in typical warm partially ionized ISM that can be successfully modeled using equilibrium photoionization models. The heliosphere wake leaves a $\sim 200 \times 1000$ AU trail in space of low density, $n < 0.05$ cm^{-3}, cooling plasma comingled with ISM. The closest ISM flows through the solar vicinity at $V_{\rm LSR} \sim 20$ km s^{-1}, with an upwind direction towards the Scorpius-Centaurus Association. Clouds in this flow have thicknesses typically < 1 pc. The flow is decelerating, with velocity variations of $\sim 3-4$ km s^{-1} pc^{-1}. The α Oph sightline shows evidence of a cold, possibly tiny, cloud.

1. Introduction

Our Sun lives in what appears to be a typical warm partially ionized low column density interstellar cloud, yet the interstellar medium (ISM) within a few parsecs of the Sun shows ionization, velocity, and abundance gradients on subparsec spatial scales. The heliosphere both responds to, and creates, small scale structure in the ISM. What do we know about the small-scale structure in the surrounding cluster of cloudlets, and what does it tell us about small-scale structure in the ISM in general?

The cluster of local interstellar cloudlets (CLIC, d$<$ 30 pc) flows past the Sun at a heliocentric velocity of $V_{\rm HC} \sim 28$ km s^{-1} (§3.). Interstellar absorption lines towards stars within 10 pc have $N({\rm H^o}) = 0.1-2.0\times10^{18}$ cm^{-2} (for D^o/H^o= 1.5×10^{-5} cm^{-2}, Wood et al. 2005; Redfield & Linsky 2004a). The mean ISM density within 10 pc is $<n({\rm H^o})>\sim 0.06$ cm^{-3}. If these clouds have the same density as the parent cloud feeding ISM into the heliosphere, $n({\rm H^o})\sim 0.18$ cm^{-3} (Slavin & Frisch 2002, 2006, SF02,SF06), then cloud thicknesses are $\sim 0.22-3.1$ pc. If the width of the observed components is formed by a mass-dependent thermal component and a mass-independent turbulent component, then cloud temperatures range between 1700 K and 12,600 K (Redfield & Linsky 2004b).

The success of equilibrium photoionization models (SF02,SF06) in predicting the properties of the Local Interstellar Cloud (LIC) surrounding the Sun suggests that clouds within 10 pc may be in pressure equilibrium with each other and with the LIC, and have similar ionization levels (§4.). In this case, the cloud densities are $n({\rm H^o}) = 0.13 - 0.97$ cm^{-3}, the cloud thicknesses are $0.06 - 2.2$ pc, and the components fill 7% to 71% of the individual sightlines. The highest filling factor would then be towards α Aql (5 pc), $\sim 80^\circ$ from the LSR upwind direction of the CLIC (§3.), which is consistent with a CLIC affiliation with an expanding evolved superbubble shell (§3.).

The heliosphere boundary conditions vary over time-scales of $10^3 - 10^5$ years because of the velocity and ionization gradients of the CLIC (§3.,4.). The Sun appears to have entered the CLIC within the past $\sim 100,000$ years, influencing the galactic cosmic ray (GCR) flux at the Earth (Frisch & Slavin 2006a,b, FS06). The paleoclimate record of short-lived radioisotopes resulting from GCR temporal variations is an in situ probe of small scale ISM structure. Interstellar dust and gas properties inside of the heliosphere depend on the heliosphere boundary conditions. Large grains and neutrals from the surrounding Local Interstellar Cloud (LIC) penetrate and interact with the solar wind plasma (§4.).

2. Solar Wake: Tiny Clump of Cooling Plasma and Hot Neutrals

The interaction between ISM and the heliosphere must generate small-scale structure in the ISM because the relative Sun-cloud motion, $\sim$26.4 km s^{-1}, generates a wake of comingled ISM and cooling solar wind that trails the Sun through space. Our Sun looses $\sim 2 \times 10^{-14}$ $M_{\rm sun}$ per year. Voyager 1, which is now exiting the heliosphere in a direction roughly towards BD+12 3139, detected the solar wind termination shock [1] at 95 AU in a direction offset $\sim 30^\circ$ away from the heliosphere nose and 34.7° above the ecliptic plane. The relative velocity of the Sun and surrounding interstellar cloud is 26.4 km s^{-1} (Witte 2004), so that for a solar wind density of $\sim$6 particles cm^{-3} at 1 AU, the solar wind leaves a trail in space of cooling solar wind material with average density ~ 0.05 cm^{-3}. The length of this solar wake, $\sim 10^3$ AU, is limited by the reconnection rate in the solar wind and charge-exchange between solar wind protons and interstellar H (Yu 1974). The $\sim 200 \times 10^3$ AU solar wake has an aspect ratio of $\sim 1/5$. Random sightlines through the solar wake will yield column densities of energetic neutral hydrogen atoms (ENAs), created by charge exchange between the solar wind and low velocity interstellar H-atoms, of $N({\rm H^o}) < 8 \times 10^{14}$ cm^{-2}. The full-width-half-max of these features should be less than twice the solar wind speed, or generally < 500 km s^{-1} for slow solar wind with higher flux levels. Such features could be a significant contaminant of the damping wings of the Lα line towards other stars. Similar features should form around other cool stars embedded in the low densities of the Local Bubble.

3. Kinematics of ISM Flow Past Sun

It was recognized long ago that the ISM inside of the solar system is part of an outflow of ISM from the Scorpius-Centaurus Association (SCA, Frisch 1981). In the local standard of rest (LSR), [2] the bulk flow of the CLIC corresponds to an upwind velocity vector $V_{\rm LSR} = -19.5 \pm 4.5$ km s^{-1}, from the direction ℓ=331°, b=–5°(Frisch et al. 2002). Ultraviolet (UV) and optical absorption lines trace

[1] The termination shock of the solar wind, where the solar wind becomes subsonic, is observed as a low energy flux of "termination shock particles" (protons), and the factor of ~ 3 compression of the solar wind magnetic field (Stone et al. 2005; Burlaga et al. 2005).

[2] We follow the practice of radio astronomers and use the Standard solar apex motion to calculate CLIC LSR velocities; see FS6 for values based on Hipparcos data).

the radial velocities of CLIC components, and indicate the flow is decelerating by $\sim 30-40$ km s^{-1} over the nearest ± 5 pc, averaging to $\sim 3-4$ km s^{-1} pc^{-1}. The most negative velocity components in the upwind direction ($V_{\rm HC}\sim -35$ to -40 km s^{-1}) approach the Sun more rapidly than the most positive velocity components in the downwind direction ($V_{\rm HC}\sim +20$ km s^{-1}) recede (Fig. 1). The velocity dispersion of ± 4.5 km s^{-1} arises partly because several individual cloudlets are identified in this flow, with LSR velocities of –20.7 km s^{-1} to –24.5 km s^{-1} and similar upwind directions (within 25° of each other, for Standard solar apex motion). The extremes of the observed velocity range are seen in stars within 5 pc of the Sun, including α Aql (5 pc) in the upwind direction and α CMa (2.7 pc) in the downwind direction (e.g. Lallement et al. 1986; Frisch et al. 2002).

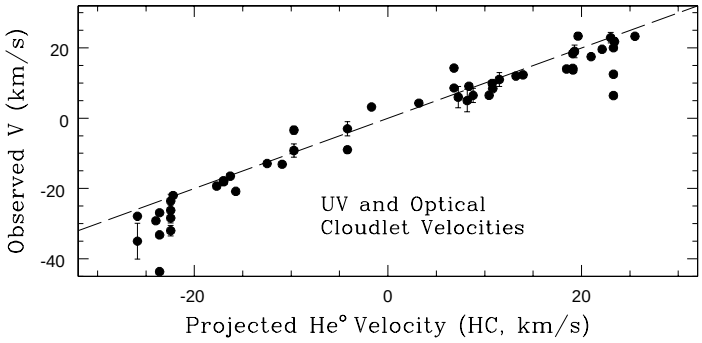

Figure 1. The observed heliocentric velocity (y-axis) of cloudlets making up the CLIC are plotted in the rest frame of the LIC (x-axis), which is defined by measurements of interstellar He$^{\rm o}$ inside of the heliosphere (§4.). The components displayed in this figure are observed towards stars within 30 pc of the Sun (see Frisch et al. 2002, for star list). Note that the CLIC flow is decelerating.

One nearby cloudlet is the Apex cloud (in the direction of solar apex motion), which is seen towards α Aql and α Oph (14 pc) with a density $n >5$ cm^{-3} if ionization is uniform (Frisch 2003). The Apex cloud also provides the only evidence for possible cold ISM close to the Sun. An H$^{\rm o}$ 21-cm absorption feature at the Apex Cloud velocity ($V_{\rm LSR} = -14$ km s^{-1}) is seen towards the radio source NVSS J1732+125, 41 arcmin (0.1 pc) from the α Oph sightline, with spin temperature $T_{\rm spin} = 40$°K and N(H$^{\rm o}$)= $10^{19.70}$ cm^{-2} (Mohan et al. 2001). Although the radio component may be beyond α Oph, the Ti$^+$ absorption at the same velocity gives $N({\rm Ti}^+)/N({\rm H}^{\rm o})\sim 10^{-9.6}$, which is within the uncertainties of similar values found for higher column density gas (Frisch et al., in preparation). The cloud length is ~ 0.16 pc for $n \sim 100$ cm^{-3}.

The physical basis of the CLIC kinematics is unknown. Possible processes include that the Sun is in a fragment of the SCA superbubble shell (Frisch 1995), that the flow results from a Rayleigh-Taylor instability in the interaction region between the Loop I supernova remnant and Local Bubble (Breitschwerdt et al. 2000), and that local ISM is caused by magnetic tension which has caused the

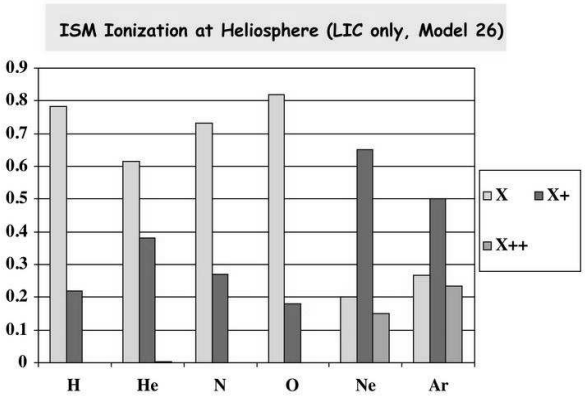

Figure 2. Ionization levels of the LIC WPIM at the Sun, based on Model 26 in the LIC-only radiative transfer models of SF06. For this model at the solar location, $n(\mathrm{He^o})$=0.015 cm^{-3}, $n(\mathrm{H^o})\sim$ 0.019 cm^{-3}, $n(\mathrm{e})\sim$ 0.06 cm^{-3}, and the fractional ionizations of H and He are $\sim$ 0.22 and $\sim$ 0.38, respectively. Other models with slightly different values are also acceptable (SF06).

detachment of a magnetic flux-tube from the Loop I bubble (Cox & Helenius 2003).

The warm partially ionized (WPIM) CLIC appears similar to warm neutral material (WNM) detected by H^o 21-cm observations (Heiles & Troland 2003), where WNM temperatures range up to $\sim$ 5000 K and $\sim$25% of the H^o mass appears at velocities $|V_{\rm LSR}| > 10$ km s^{-1}. The LIC heliocentric velocity measured from the detection of interstellar He^o inside of the solar system is –26.3 km s^{-1} (Witte 2004), which should not be surprising since encounters between the Sun and ISM with a relatively high Sun-cloud velocities are more likely.

4. Ionization: The Heliosphere Vantage Point

Observations of ISM inside of the heliosphere provides a unique opportunity to constrain the physical properties of the ISM at a single location in space using radiative transfer models to reconstruct ionization gradients that are present in WPIM. Generally, absorption line data sample ISM velocity structure blended over large distances, masking small scale structure related to ionization gradients. Elements with first ionization potentials (FIP) $\geq$ 13.6 eV are partially ionized since an opacity of $\tau \sim 1$ for H and He ionizing photons is achieved for $N(\mathrm{H^o})\sim 10^{17.3}$ cm^{-2} and $N(\mathrm{H^o})\sim 10^{17.7}$ cm^{-2}, respectively. The resulting ionization gradients, including for H^o/He^o, requires radiative transfer models to recover cloud properties at any single location (SF02,SF06). Observations of interstellar neutrals and their byproducts inside of the heliosphere diagnose the ionization levels. Among partially ionized elements detected in the heliosphere are He, O, N, Ne, and Ar.

ISM types measured inside of the heliosphere include large dust grains (radii > 0.15 μm), He^o atoms (e.g. Witte 2004), measurements of solar Lα and 584 A florescence from H^o and He^o, and measurements of H, He, O, N, Ne, and Ar "pickup ions" and "anomalous" cosmic rays (PUI, ACR, e.g. Cummings et al. 2002; Möbius et al. 2004; Gloeckler & Geiss 2004).[3] Densities at the termination shock of the parent neutral interstellar atoms can be derived from PUI and ACR data, after correction for ionization and propagation processes. These densities are corrected to interstellar values through calculations of possible loss in the heliosheath due to charge exchange or electron impact ionization processes, termed "filtration". Fig. 2 shows the relative ionizations of the LIC, which forms the PUI parent population.

Interstellar He^o at the Sun has density n(He^o)= 0.015 cm^{-3}, temperature $T = 6400$ K, and heliocentric velocity –26.3 km s^{-1}(Witte 2004). The observed n(He^o) value serves as a strong constraint on the SF02 and SF06 radiative transfer photoionization models that predict the ISM properties close to the Sun. However, H^o data are less useful because up to 50% of interstellar H is lost by charge-exchange in the heliosheath regions, and H^o trajectories depend on $\beta = \frac{F_{\rm Radiation}}{F_{\rm Gravitation}}$, which is solar cycle dependent (> 1 during solar maximum and ~ 1 during minimum).

Table 1. Comparisons between ISM at the Sun and other nearby PWIM

Ratio	Local ISM (N(X) ratios)	PUI at the TS[1] (n(X) ratios)	ISM at Sun Model 26, SF06 (n(X) ratios)
H^o/He^o	12.8 ± 1.4[2]	6.8 (9.9)[3]	12.4
O^o/N^o	8.7[4]	8.8	7.3
O^o/H^o	0.00040[4]	0.00047	0.00033
Ar^o/O^o	0.0039 or < 0.0016[4,5]	0.0034	0.0026[6]
Ne^o/He^o	–	0.00041	0.00040[7]

[1] The H, O, and N PUI n(X) (cm^{-3}) values at the termination shock (TS) should be corrected by ~ 1.45, 1.32, and ~ 1.22, respectively, to recover interstellar values because of filtration losses in heliosheath regions. [2] Based on column density (N(X), cm^{-2}) data for five white dwarf stars 50–79 pc from the Sun (e.g. Wolff et al. 1999). [3] The ratio is parentheses is derived from observations of the H^o Lα backscatter measurements inside of the heliosphere. [4] Column densities (N(X), cm^{-2}) from Lehner et al. (2003) for stars within 70 pc. [5] The observed Ar^o/O^o distribution appears to be bimodal, with small values representing highly ionized gas. [6] This value is based on an abundance Ar/H=2.82 ppm. [7] This value is based on an abundance Ne/H=123 ppm.

Table 1 compares interstellar element ratios found from column density data (N, cm^{-2}) towards nearby stars (column 2), volume density (n, cm^{-3}) ratios at the solar wind termination shock, with predictions of the RT Model

[3]PUIs are formed by charge exchange between interstellar neutrals and the solar wind. These low energy ions are captured by the solar wind and convected outwards, where they are accelerated beyond the termination shock to low cosmic ray energies, < 500 MeV/nucleon, forming ACRs.

26 from SF06. Once filtration corrections are applied to the PUI H, N, and O data, all three sets of data are in good agreement indicating that ISM at the Sun has similar abundances and ionizations as other ISM within 50–70 pc. The exception is the sightline towards HD 149499B, 37 pc away in the LSR upwind direction (ℓ,b=330°,–7°), which is $\sim$ 67% ionized and may trace an extended nearby HII region. Enhanced $N(Fe^+)/N(D^o)$ ratios in the LSR upwind direction also suggest a local ionization source (FS06). Otherwise, the LIC ionization level is heavily dominated by the primary ionization sources in the third and fourth galactic quadrants (ℓ=180°–270°–360°), corresponding to regions of the Local Bubble within $\sim$ 150 pc that have low average interstellar opacities for $\lambda < 1500$ A (Frisch, in preparation).

Acknowledgments. P. Frisch would like to thank Jon Slavin for helpful conversations. This research is supported by NASA grants NAG5-13107 and NNG05GD36G.

References

Breitschwerdt, D., Freyberg, M. J., & Egger, R. 2000, A&A, 361, 303
Burlaga, L. F., Ness, N. F., Acuña, M. H., Lepping, R. P., Connerney, J. E. P., Stone, E. C., & McDonald, F. B. 2005, Science, 309, 2027
Cox, D. P. & Helenius, L. 2003, ApJ, 583, 205
Cummings, A. C., Stone, E. C., & Steenberg, C. D. 2002, ApJ, 578, 194
Frisch, P. C. 1981, Nat, 293, 377
—. 1995, Space Sci.Rev., 72, 499
—. 2003, ApJ, 593, 868
Frisch, P. C., Grodnicki, L., & Welty, D. E. 2002, ApJ, 574, 834
Frisch, P. C. & Slavin, J. D. 2006a
—. 2006b, Astrophysics and Space Sciences Transactions, 2, 53
Gloeckler, G. & Geiss, J. 2004, Advances in Space Research, 34, 53
Heiles, C. & Troland, T. H. 2003, ApJ, 586, 1067
Lallement, R., Vidal-Madjar, A., & Ferlet, R. 1986, A&A, 168, 225
Lehner, N., Jenkins, E., Gry, C., Moos, H., Chayer, P., & Lacour, S. 2003, ApJ, 595, 858
Möbius, E., Bzowski, M., Chalov, S., Fahr, H.-J. et al 2004, A&A, 426, 897
Mohan, R., Dwarakanath, K. S., Srinivasan, G., & Chengalur, J. N. 2001, Journal of Astrophysics and Astronomy, 22, 35
Redfield, S. & Linsky, J. L. 2004a, ApJ, 602, 776
—. 2004b, ApJ, 613, 1004
Slavin, J. D. & Frisch, P. C. 2002, ApJ, 565, 364
—. 2006, ApJ, in preparation
Stone, E. C., Cummings, A. C., McDonald, F. B., Heikkila, B. C., Lal, N., & Webber, W. R. 2005, Science, 309, 2017
Weller, C. S. & Meier, R. R. 1981, ApJ, 246, 386
Witte, M. 2004, A&A, 426, 835
Wolff, B., Koester, D., & Lallement, R. 1999, A&A, 346, 969
Wood, B. E., Redfield, S., Linsky, J. L., Müller, H.-R., & Zank, G. P. 2005, ApJS, 159, 118
Yu, G. 1974, ApJ, 194, 187